

Virginia Transportation Research Council

research report

Using Fiber-Optic Sensor Technology to Measure Strains Under the Asphalt Layer of a Flexible Pavement Structure

http://www.virginia.gov/vtrc/main/online_reports/pdf/07-r5.pdf

STEPHEN R. SHARP, Ph.D.

Research Scientist

Virginia Transportation Research Council

KHALED A. GALAL, Ph.D.

Research Scientist

Virginia Transportation Research Council

MOHAMED K. ELFINO, Ph.D., P.E.

Assistant State Materials Engineer

Virginia Department of Transportation



Standard Title Page - Report on State Project

Report No. VTRC 07-R5	Report Date August 2006	No. Pages 43	Type Report: Final Period Covered:	Project No.: 69827 Contract No.
Title: Using Fiber-Optic Sensor Technology to Measure Strains Under the Asphalt Layer of a Flexible Pavement Structure			Key Words: FWD, falling weight deflectometer, fiber-optic, HMA, multi-layer elastic analysis, pavement, sensor, strain	
Authors: Stephen R. Sharp, Khaled A. Galal, and Mohamed K Elfino				
Performing Organization Name and Address: Virginia Transportation Research Council 530 Edgemont Road Charlottesville, VA 22903				
Sponsoring Agencies' Name and Address Virginia Department of Transportation 1401 E. Broad Street Richmond, VA 23219				
Supplementary Notes				
<p>Abstract</p> <p>In this study, a flexible pavement system was instrumented using fiber-optic strain sensors (FOSS). The purpose of this study was to demonstrate the feasibility of a FOSS installation, monitor the long-term strains under repeated traffic loading, and compare the measured strains with the calculated ones from multi-layer elastic (MLE) analysis.</p> <p>MLE analysis was performed before and after FOSS installation to monitor strains during and after construction. In-situ strains during construction under the hot-mix asphalt (HMA) delivery truck, paver operations, and roller operations were compared to the results of theoretical MLE analysis. In addition, in-situ strains after construction under dump truck and falling weight deflectometer (FWD) loadings at multiple load levels were compared to the results of theoretical and in-situ MLE analysis.</p> <p>The in-situ strain under construction was at least 50 fold that obtained with MLE analysis. The FOSS were sensitive enough to collect strain measurements during construction at very high construction temperatures and moisture conditions. Further, the MLE analysis results were very close to the measured deflection under dump truck and FWD loadings.</p> <p>The results show that MLE analysis can be used to validate and calculate the strains in asphalt pavement sections. Long-term performance monitoring is continuing, and the study will be repeated after FOSS placement in new HMA pavement sections.</p> <p>Understanding the behavior of asphalt pavement under repeated traffic loads can result in an optimized design, thus reducing the rehabilitation costs associated with premature failures or the higher costs associated with conservative asphalt pavement designs. The in-situ strains can be used to calibrate mechanistic-empirical pavement design guide (MEPDG) performance models for local conditions so that measurements can better predict the life of pavement layers and the layers that will need replacement. The installation of FOSS at selected pavement sites that represent the typical pavement designs across the state would allow for the development of accurate statewide mechanistic-empirical performance models, which would lead to more cost-effective pavement rehabilitation decisions.</p>				

FINAL REPORT

**USING FIBER-OPTIC SENSOR TECHNOLOGY TO MEASURE STRAINS UNDER
THE ASPHALT LAYER OF A FLEXIBLE PAVEMENT STRUCTURE**

Stephen R. Sharp, Ph.D.
Research Scientist
Virginia Transportation Research Council

Khaled A. Galal, Ph.D.
Research Scientist
Virginia Transportation Research Council

Mohamed K. Elfino, Ph.D., P.E.
Assistant State Materials Engineer
Virginia Department of Transportation

Virginia Transportation Research Council
(A partnership of the Virginia Department of Transportation and
the University of Virginia since 1948)

Charlottesville, Virginia

August 2006
VTRC 07-R5

DISCLAIMER

The contents of this report reflect the views of the authors, who are responsible for the facts and the accuracy of the data presented herein. The contents do not necessarily reflect the official views or policies of the Virginia Department of Transportation, the Commonwealth Transportation Board, or the Federal Highway Administration. This report does not constitute a standard, specification, or regulation.

Copyright 2006 by the Commonwealth of Virginia.

ABSTRACT

In this study, a flexible pavement system was instrumented using fiber-optic strain sensors (FOSS). The purpose of this study was to demonstrate the feasibility of a FOSS installation, monitor the long-term strains under repeated traffic loading, and compare the measured strains with the calculated ones from multi-layer elastic (MLE) analysis.

MLE analysis was performed before and after FOSS installation to monitor strains during and after construction. In-situ strains during construction under the hot-mix asphalt (HMA) delivery truck, paver operations, and roller operations were compared to the results of theoretical MLE analysis. In addition, in-situ strains after construction under dump truck and falling weight deflectometer (FWD) loadings at multiple load levels were compared to the results of theoretical and in-situ MLE analysis.

The in-situ strain under construction was at least 50 fold that obtained with MLE analysis. The FOSS were sensitive enough to collect strain measurements during construction at very high construction temperatures and moisture conditions. Further, the MLE analysis results were very close to the measured deflection under dump truck and FWD loadings.

The results show that MLE analysis can be used to validate and calculate the strains in asphalt pavement sections. Long-term performance monitoring is continuing, and the study will be repeated after FOSS placement in new HMA pavement sections.

Understanding the behavior of asphalt pavement under repeated traffic loads can result in an optimized design, thus reducing the rehabilitation costs associated with premature failures or the higher costs associated with conservative asphalt pavement designs. The in-situ strains can be used to calibrate mechanistic-empirical pavement design guide (MEPDG) performance models for local conditions so that measurements can better predict the life of pavement layers and the layers that will need replacement. The installation of FOSS at selected pavement sites that represent the typical pavement designs across the state would allow for the development of accurate statewide mechanistic-empirical performance models, which would lead to more cost-effective pavement rehabilitation decisions.

FINAL REPORT

USING FIBER-OPTIC SENSOR TECHNOLOGY TO MEASURE STRAINS UNDER THE ASPHALT LAYER OF A FLEXIBLE PAVEMENT STRUCTURE

Stephen R. Sharp, Ph.D.
Research Scientist
Virginia Transportation Research Council

Khaled A. Galal, Ph.D.
Research Scientist
Virginia Transportation Research Council

Mohamed K. Elfino, Ph.D., P.E.
Assistant State Materials Engineer
Virginia Department of Transportation

INTRODUCTION

Pavement performance is specifically related to design, evaluation, construction, and management, and it is usually predicted through performance prediction equations commonly known as transfer functions. Transfer functions relate different pavement distresses and pavement responses (stresses, strains, and/or deflections), allowing the computation of the number of load applications to failure. This number is a function of pavement responses (and materials properties) at critical pavement locations.

One of the most critical locations for hot-mix asphalt (HMA) or flexible pavements is the bottom of the asphalt pavement layer. It has been well established that the measured radial tangential strains (tensile strain) at the bottom of the asphalt layer is directly related to the fatigue life of asphalt pavement (Huang, 1993). Thus, measuring or predicting the in-situ tensile strain at the bottom of the asphalt layer is important to predict fatigue life. Knowing the tensile strain at this critical location, along with the resilient or dynamic modulus of the asphalt layer, in some cases, enables the prediction of the number of load repetitions to pavement failure. Vertical compressive strains on the top of the subgrade of the asphalt pavement are another important pavement response to predict the potential subgrade rutting in HMA pavements.

Several fatigue and rutting asphalt transfer functions have been developed to relate the asphalt modulus and/or the measured strain under the asphalt layers to the number of load repetitions to pavement failure. Fatigue transfer functions take one of two basic forms that represent most developed fatigue damage models (Huang, 1993; Thompson et al., 1989; Federal Highway Administration [FHWA], 1995):

$$N_f = f_i (C_i)^{-j^2} \quad (\text{Eq. 1})$$

$$N_f = f_1 (C_t)^{f_2} (E)^{f_2} \quad (\text{Eq. 2})$$

where

N_f = number of allowable load repetitions to fatigue failure
 f_1, f_2 = regression constants
 C_t = tensile strains at the bottom of the asphalt layer
 E = asphalt modulus.

Rutting in asphalt pavements is represented by two types of transfer functions: subgrade rutting and asphalt rutting. The transfer equations of the subgrade rutting take the following basic form (Huang 1993):

$$N_f = f_1 (\varepsilon_v)^{f_2} \quad (\text{Eq. 3})$$

where

N_f = number of allowable load repetitions to subgrade rutting failure
 f_1, f_2 = regression constants
 ε_v = vertical compressive stresses at the top of the subgrade layer.

HMA pavement rutting transfer functions take the following basic form (Huang, 1993, Thompson et al., 1989; FHWA, 1995):

$$\log \varepsilon_p = a + b (\log N) \quad (\text{Eq. 4})$$

where

N = number of allowable load repetitions to material rutting failure
 A = experimentally established parameter, depends on material and stress state conditions
 B = experimentally established parameter, usually varies between 0.1 and 0.2
 ε_p = permanent strain.

Table 1 summarizes several commonly used transfer functions for predicting asphalt fatigue and subgrade rutting in HMA pavements (Huang, 1993; Thompson et al., 1989; FHWA, 1995).

Theoretical predictions of pavement responses (stresses, strains and deflections) in HMA pavements are typically obtained using several methods: multi-layer elastic (MLE) analysis, non-linear elastic analysis, and/or finite element modeling. The latter was reported to be one of the most accurate methods to predict pavement responses under dynamic loading (Uddin, 1998; Uddin and Godiwalla, 1998; Uddin, 2000; Uddin et al., 2003). However, many studies have documented that MLE or non-linear elastic analysis results are quite accurate for the purpose of predicting pavement performance under dynamic loading using MLE static analysis (Uddin, 1998; Uddin and Godiwalla, 1998; Uddin, 2000; Uddin et al., 2003; Ullidtz, 1998).

Table 1. Common Asphalt Pavements Transfer Functions Used in United States (FHWA, 1995)

Method	Transfer Function
<i>Fatigue Models</i>	
Asphalt Institute Design Method	$N_f = 0.0796 (\epsilon_t)^{-3.291} (E)^{-0.854}$
Shell Pavement Design Manual (1978)	$N_f = 0.0685 (\epsilon_t)^{-5.671} (E)^{-2.363}$
Illinois Department of Transportation	$N_f = 5.0 \times 10^{-6} (\epsilon_t)^{-3.0}$
PDMAP (10%)	$\log N_f(10\%) = 15.947 - 3.291 \log (\epsilon / 10^{-6}) - 0.854 \log (E / 10^3)$
PDMAP (45%)	$\log N_f(45\%) = 16.086 - 3.291 \log (\epsilon / 10^{-6}) - 0.854 \log (E / 10^3)$
UK Transport and Road Research Lab	$N_f = 1.66 \times 10^{-10} (\epsilon_t)^{-4.32}$
Belgian Road Research Center	$N_f = 4.92 \times 10^{-14} (\epsilon_t)^{-4.76}$
<i>Subgrade Rutting Models</i>	
Asphalt Institute Design Method	$N_f = 1.365 \times 10^{-9} (\epsilon_v)^{-4.477}$
Shell Pavement Design Manual (revised 1985)	$N_f = 6.15 \times 10^{-7} (\epsilon_v)^{-4.0}$ (50% reliability)
Shell Pavement Design Manual (revised 1985)	$N_f = 1.94 \times 10^{-7} (\epsilon_v)^{-4.0}$ (85% reliability)
Shell Pavement Design Manual (revised 1985)	$N_f = 1.05 \times 10^{-7} (\epsilon_v)^{-4.0}$ (95% reliability)
UK Transport and Road Research Lab	$N_f = 6.18 \times 10^{-8} (\epsilon_v)^{-3.95}$
Belgian Road Research Center	$N_f = 3.05 \times 10^{-9} (\epsilon_v)^{-4.35}$

Installing pavement sensors that accurately measure the strains under the asphalt pavement layer is one of the most accurate ways to predict pavement performance under traffic loadings (Loulizi et al., 2002; Al-Qadi et al., 2004). These measurements can also be used to develop new pavement performance prediction models over a long period of time. Most of the sensors used in pavement instrumentation are reported to have a limited in-service life that usually varies between 1 and 5 years (Loulizi et al., 2002; Al-Qadi et al., 2004).

Fiber-optic strain sensors (FOSS) are a new technology that holds the promise of allowing long-lasting strain monitoring during the in-service life of pavements. Sharp et al. (2005) reported that FOSS can be installed in asphalt pavement layers, allowing for continuous strain measurement under real-time pavement traffic loading.

BACKGROUND

Studies have shown that FOSS provide additional benefits over traditional strain-measuring devices. They can measure both static and dynamic loading (i.e., are frequency independent (Safaai-Jazi et al., 1990), provide precise quantitative strain data (Masri et al., 1994), display superior corrosion resistance, and are unaffected by electromagnetic fields (de Vries et al., 1996). However, as shown in Table 2, various types of fiber-optic sensing technology are currently available. Therefore, it is important to determine which type best matches the criteria determined for a particular application. For this project, an extrinsic Fabry-Perot interferometer (EFPI) FOSS was selected based on the comparison by de Vries et al. (1994) because it provides an excellent balance among sensitivity, frequency response, and cost.

Table 2. Examples of Different Types of Fiber-Optic Sensors

Coupler-based	Liquid-core Fibers
E-core, 2 mode	Michelson
Extrinsic	Mach-Zehnder
Fabry-Perot (Intrinsic)	OTDR (Fresnel)
Fabry-Perot (Extrinsic)	OTDR (Rayleigh)
Grating-based (Bragg) Reflector	Polarimetric, Twin Core

After the type of fiber-optic sensor was selected, a FOSS design that allowed for placement during pavement construction with minimal disruption to the construction processes was successfully tested and completed in an earlier phase of this research project (Sharp et al., 2005). The current project was launched with the placement of the EFPI FOSS in an actual asphalt pavement structure and a subsequent evaluation of in-situ strain in that structure.

PURPOSE AND SCOPE

As stated previously, there is a need to measure the strain under asphalt pavement layers and the pavement responses, i.e., stresses, strains, and deflections, at critical pavement locations. Thus, the major objectives of this study were as follows.

1. Document the FOSS installation and calibration process.
2. Verify, monitor, and document the strains under the loadings of construction equipment and selected temperatures based on theoretical MLE analysis predictions.
3. Determine the effect/impact of the FOSS on the measured stiffness of the different pavement layers by comparing the stiffness of the pavement layers with and without FOSS.
4. Verify, monitor, and document the strains under FWD loadings and dump truck loadings (DTL) just after construction, and compare the strains measured with the strains predicted by the MLE analysis.
5. Describe the future work that will be conducted to validate the results and the sensitivity of FOSS on asphalt pavement.

METHODOLOGY

Overview

Four tasks were conducted to achieve the study objectives:

1. site selection and preparation

2. FOSS calibration and installation
3. initial installation testing and measurements under HMA delivery truck, paver, and roller loadings
4. post-construction testing using DTL and FWD deflection testing at various load levels.

Predicted Theoretical and In-Situ Pavement Strain

Using the MLE analysis program ELSYM5, the theoretical predicted stresses, strains, and deflections were calculated for the selected pavement section by defining the modulus of each pavement layer, the thickness of each pavement layer, and the corresponding Poisson's ratio of each pavement layer.

The cross section of the instrumented pavement used in this study is shown in Figure 1 and consisted of the following layers: 9.5 in of dense-graded HMA layer(s), (1.5 in of HMA surface, 2 in of HMA intermediate mix, and 6 in of HMA densely graded base layer); 3 in of asphalt-treated open-graded drainage layer (OGDL); 7 in of cement-treated aggregate (CTA) base layer; 6 in of dense-graded aggregate base layer; and a semi-infinite subgrade layer that represents both compacted subgrade soil and natural subgrade soils. A weathered shale rock layer was observed near the top of the subgrade along the pavement section. The depth of this layer varied along the pavement section, with a shallow depth near the end of the experimental section.

Table 3 shows the typical modulus value for each pavement layer, based on traditionally observed values in Virginia, corresponding thickness, and Poisson's ratio of each pavement layer. These data were used at different load levels to predict the pavement responses.

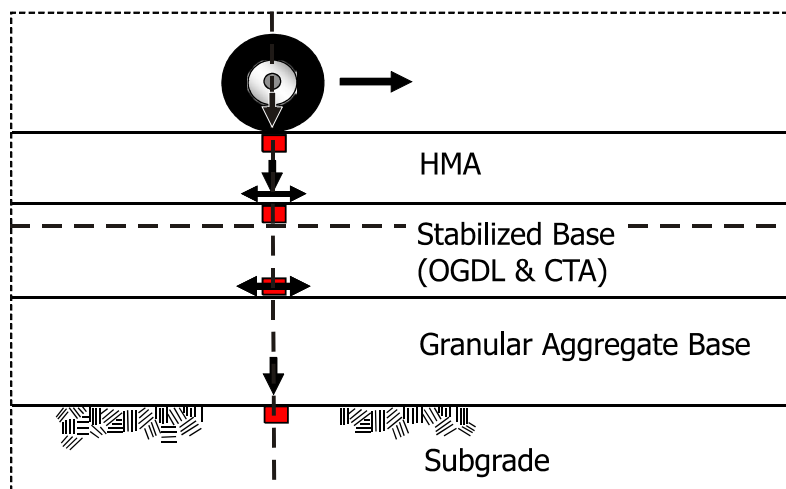


Figure 1. Instrumented Pavement Cross Section of Route 29 Bypass Near Lynchburg. HMA = hot-mix asphalt, OGDL = open-graded drainage layer, CTA = cement-treated aggregate.

Table 3. Pavement Layer Moduli, Corresponding Thicknesses, and Poisson's Ratio Used to Predict Theoretical Pavement Strains

Material	Thickness	Poisson's Ratio	Typical Modulus Value (psi)
Asphalt layer	9.5	0.35	400,000-3,500,000
Open-graded drainage layer	3	0.35	100,000-300,000
Cement-treated aggregate base	7	0.2	100,000-1,200,000
Dense-graded aggregate layer	6	0.35	30000-80,000
Compacted subgrade soil		0.35	5,000-20,000

Note: Weathered shale rock has the following ranges: Poisson's ratio, 0.2; typical modulus, 50,000-150,000.

The major objective of predicting the theoretical pavement response (and subsequently the in-situ pavement responses) was to use it as a "preliminary" evaluation/indicator of the in-situ FOSS measurements. The predicted theoretical values were hypothesized to be in close proximity to the measured strain values after construction under simulated traffic loading.

MLE analysis was used to verify and validate the FOSS readings. First, MLE analysis based on theoretical layer moduli was used to verify the initial FOSS readings during installation and construction. Then, MLE analysis based on the in-situ backcalculated layer moduli was used to compare the MLE strain results with those under dump truck and FWD loadings.

Site Selection and Installation of FOSS

A pavement section nearing the construction stage on the Route 29 Bypass near Lynchburg, Virginia, was selected for this study. Twenty calibrated FOSS were installed in the south travel lane of the bypass, which is approximately 2 mi north of Route 460. This section of the highway was built on variable shale rock depths and was constructed in accordance with Virginia Department of Transportation (VDOT) standards with all preparation work following normal VDOT construction procedures. The plan and section views are shown in Figures 2 and 3, respectively.

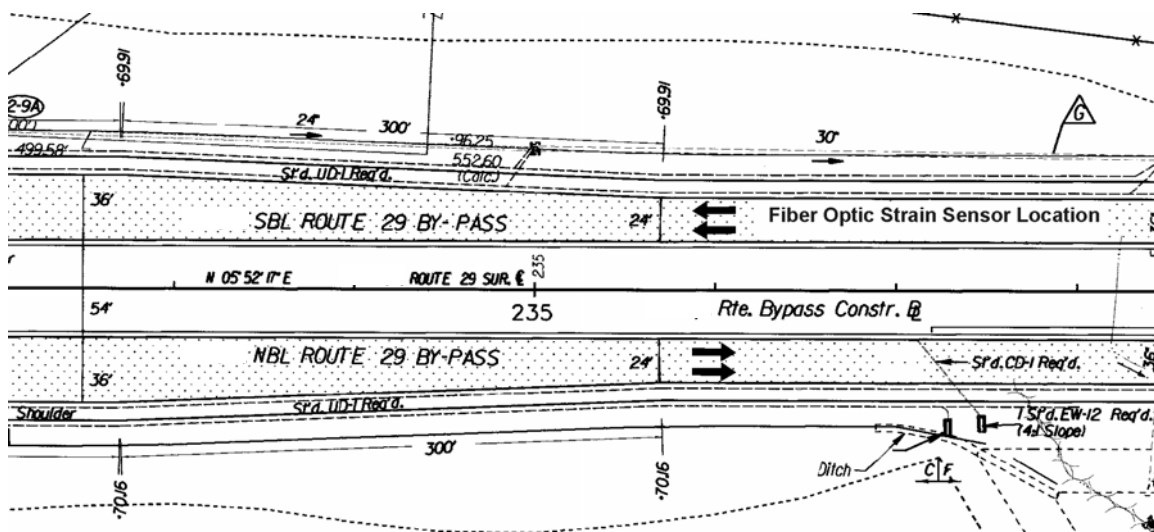
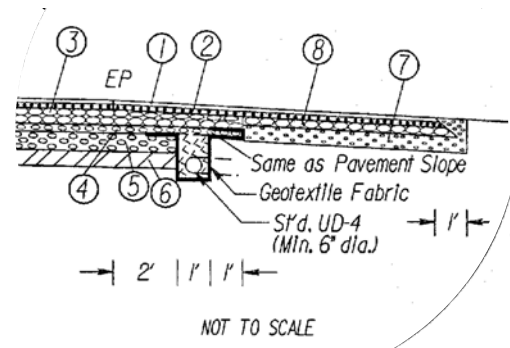


Figure 2. Route 29 Bypass Near Lynchburg, Virginia: Plan View of Region with Fiber-Optic Strain Sensors



- ① ASPHALT CONCRETE SURFACE COURSE TYPE SM-9.5D
- ② ASPHALT CONCRETE INTERMEDIATE COURSE TYPE IM-19.0D
- ③ 6" ASPHALT CONCRETE BASE COURSE TYPE BM-25
- ④ 3" ASPHALT STABILIZED OPEN-GRADED MATERIAL TYPE III
- ⑤ 7" SUBBASE MATERIAL CEMENT STABILIZED AGGREGATE, BASE MATERIAL TYPE I, NO. 21A, 4% CEMENT BY WEIGHT (PLUS 6% MOISTURE WITH PRIME & COVER MATERIAL)
- ⑥ 6" AGGREGATE BASE MATERIAL TYPE I NO. 21B
- ⑦ 6" AGGREGATE BASE MATERIAL TYPE I NO. 21B
- ⑧ 4" ASPHALT CONCRETE BASE COURSE TYPE BM-25

Figure 3. Route 29 Bypass Near Lynchburg, Virginia: Section View of Pavement Structure with Fiber-Optic Strain Sensors

The FOSS were installed during the construction of the bypass between stations 232 plus/minus 00 and 238 plus/minus 00, with 10 sensors placed at the bottom of the HMA base mix and 10 at the bottom of the HMA surface mix. Further, half of each group of sensors were oriented longitudinally (parallel with the direction of travel) and the other half in the transverse direction (perpendicular to the direction of travel) in the wheel path 2 to 3 feet from the edge of the lane, as is shown in Figure 4.

The FOSS were placed longitudinally and transversely with the direction of travel to capture the strains parallel and perpendicular to the load application (i.e., the load in the Y and X directions). In addition, each sensor placed in the surface mix had the same orientation as the sensor directly below it in the base mix. Finally, the sensors were placed in *both* wheel paths of the travel lane every 50 ft.

To help embed the sensors during the paving operation, HMA was placed and lightly compacted on top of the leads and sensors prior to paving. The paving and construction operations then proceeded as normal for the base and surface mixes.

FOSS Measurements and Calibration

Initially, FOSS measurements were gathered using a FiberScan 2000 as the signal conditioning unit; however, the study team decided to switch signal conditioning units and gather data using a newly developed signal conditioning unit, the FiberPro2. The FiberPro2 was

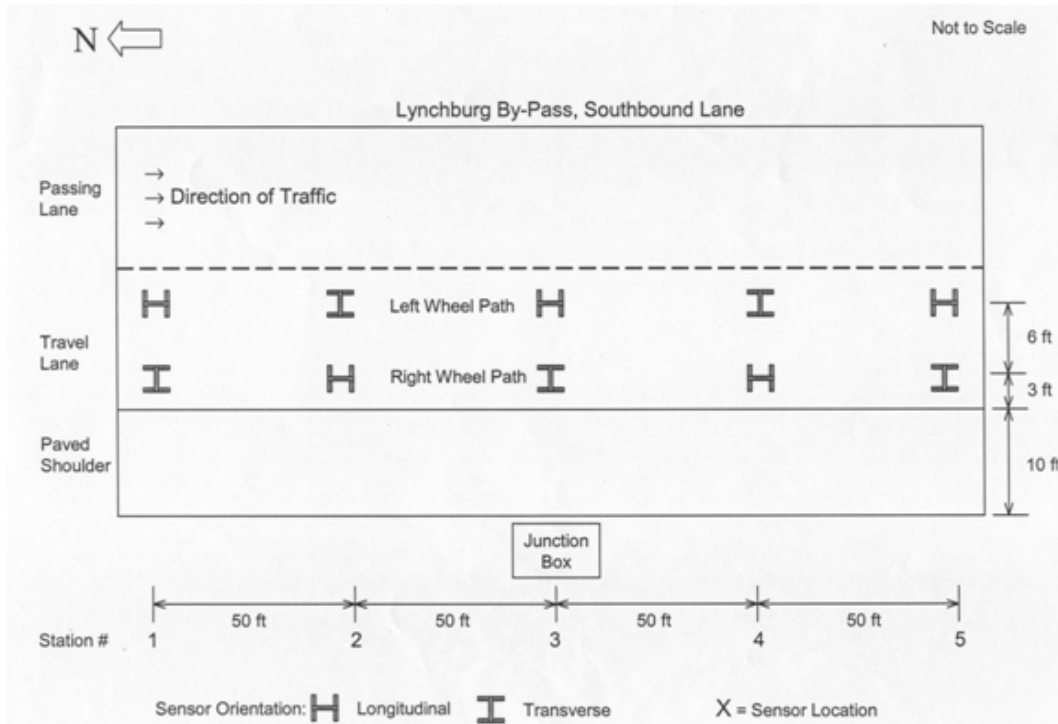


Figure 4. Location and Orientation of Fiber-Optic Strain Sensors

selected because it can interrogate the EFPI-FOSS at a higher frequency, improving the data clarity at higher test speeds. Some of the operational features for each signal conditioning unit device are listed in Table 4.

To measure the displacement using FOSS, the signal conditioning unit measures the optical path length between two reflective surfaces. These surfaces are created at each air/glass interface, which is shown in Figure 5 as R1 and R2. Therefore, a portion of the light originally transmitted from the laser to the sensor is reflected back through the fiber and optical coupler because of reflections R1 and R2. The interaction between the transmitted and reflected light creates intensity fringe patterns (shown in Figure 6), which are monitored by the detector. These patterns are related to the distance between the end of one fiber and the start of the next, which is also known as the gap length. The change in the gap length is related to the change in the sensor length through the use of a custom-designed calibration rig. The calibration rig can then be used to determine a mathematical function that relates the change in gap length to the total sensor displacement, and this function then provides the necessary relationship for an EFPI-based fiber optic sensor to measure the strain in a pavement structure. To determine the strain, the measurements were made by creating a connection between the EFPI-based FOSS and the layer of interest in the asphalt pavement.

Table 4. Operational Features of FiberScan 2000 and FiberPro2 Signal Conditioning Units

Description	FiberScan 2000	FiberPro2
Displacement resolution, nm	<1	<1
Strain resolution, microstrain	<1	<1
Strain range, microstrain	-20,000 to 20,000	-20,000 to 20,000
Refresh rate, Hz	100	960
Fiber-optic sensor types	EFPI	EFPI, Long Period Grating and Fiber Bragg Gratings

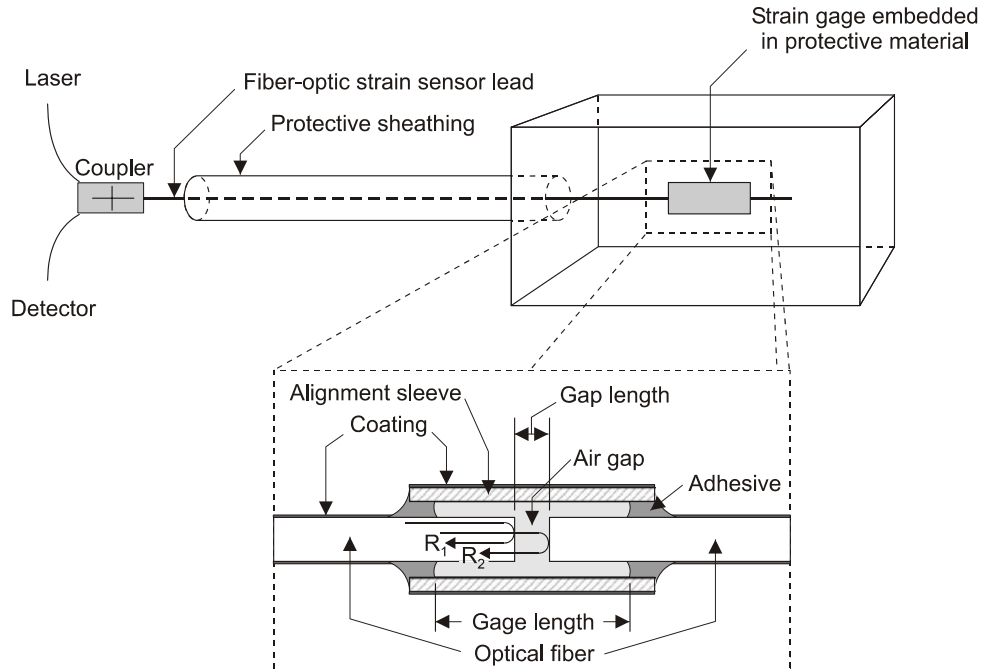


Figure 5. Schematic Showing How EFPI Fiber-Optic Sensors Function



Figure 6. Display of Intensity Fringe Patterns on Laptop Computer Screen

Initial Installation Testing and Measurements Under HMA Delivery Truck, Paver, and Roller Loadings

The first 10 FOSS were placed at the bottom of the asphalt base mix on June 9, 2004, as shown in Figure 7. The sensors were laid on top of the OGDL (i.e., drainage layer) (Figure 7A),



(A)



(B)



(C)



(D)



(E)

Figure 7. Placement of Fiber-Optic Strain Sensors Under Base Mix. (A) Sensors placed on top of open-graded drainage layer. (B) Sensors and leads covered with thin 1-inch base mix prior to paving. (C) Lead extends from roadway and is placed in shallow trench to protect leads during construction of shoulder. (D) Close-up of lead exiting roadway. (E) Sensors covered and ready for paver to place base mix layer.

covered with a thin 1-in layer of the base mix (Figure 7B), the sensor leads were allowed to drape off the edge of the stabilized drainage base, and placed in a shallow trench (Figure 7B and C). This process was repeated for all FOSS embedded in the base mixture. During this stage, strain measurements were made as the base mix was being placed.

On July 21, 2004, similar procedures were followed to place 10 more FOSS under the HMA surface layer approximately 1.5 in from the top of the finished pavement surface. In this stage, surface mixture was used to cover the FOSS instead of base mixture. The installation of the FOSS under the surface mixture and paving operations are shown in Figure 8.

After the placement and calibration of the FOSS under the HMA base mixture, two sensors were selected to monitor the strain readings during construction operations (paving and roller compaction). Unfortunately, multiple delays in placement of the surface mix created uncertainty as to when the mix would actually be placed. Therefore, the FOSS measurement technician was unable to schedule a site visit during the placement of the surface mix sensors, so measurements during the paving operation were not made.

The HMA mixes were produced at high temperatures (290 F to 300 F) and were placed at a temperature greater than 220 F to comply with VDOT's specifications and requirements. During these harsh conditions and as a result of the rolling operation, high moisture conditions can be observed at the testing site. The measured strains were expected to be several fold higher than normal strains because of the elevated temperatures and high loadings during the construction process. As explained previously, theoretical strains were computed from MLE analysis using ELSYM5 and were used to estimate the potential fiber-optics strain readings during the construction process (HMA delivery truck, paving operations, and roller operations).

Sensor Testing

It was decided that two sensors would be monitored during the placement of the base mix and then again during the placement of the surface mix. After the FOSS were embedded under the appropriate mix, each sensor was tested to determine if it was responding by having an individual jump up and down on top of the asphalt pavement directly over the sensor. A second person would monitor the detector and could quickly determine if the sensors were responding. Although this test was unsophisticated, it illustrates how sensitive FOSS are, how quickly they respond, and how easily they can be tested.

Temperature Measurements

A temperature profile at different depths of the asphalt layer was needed to explain the strain values as a function of temperature and depth. To monitor the temperature, t-type thermocouples were embedded in the surface and base mixes to monitor the temperature at these two depths (1.5 and 9.5 in from the pavement surface). In the base mix, 10 thermocouples were embedded adjacent to each sensor. In the surface mix, 7 thermocouples were embedded adjacent to each sensor.



Figure 8. Placement of Fiber-Optic Strain Sensors Under Surface Mix Layer. (A) sensors covered with surface mix. (B) Leads exit asphalt surface and are quickly embedded in shoulder material. (C) Dump trucks begin backing over sensors to fill hopper. (D) Front tire on sensor. (E) Hard rubber tire on sensor. (F) Paver tire crosses sensor. (G) Hot asphalt covers sensor. (H) Last truck fills hopper as paver crosses last strain sensor location.

Post-Construction Testing Using Dump Truck Loading and FWD Deflection Testing at Various Drop Levels

After the placement, calibration, and initial testing under construction traffic, the survivability of the FOSS was measured. Thirteen of the 20 FOSS survived the placement and construction processes; 5 were fully operational under the HMA base mix, and 8 were fully operational under the HMA surface mix in both wheel paths of the travel lane.

Two testing loading experiments were conducted; in the first, a dump truck at two (distinct-measured) load levels was used (Figure 9), and in the second, FWD impact loads were used at four load levels at both wheel paths (Figure 10).

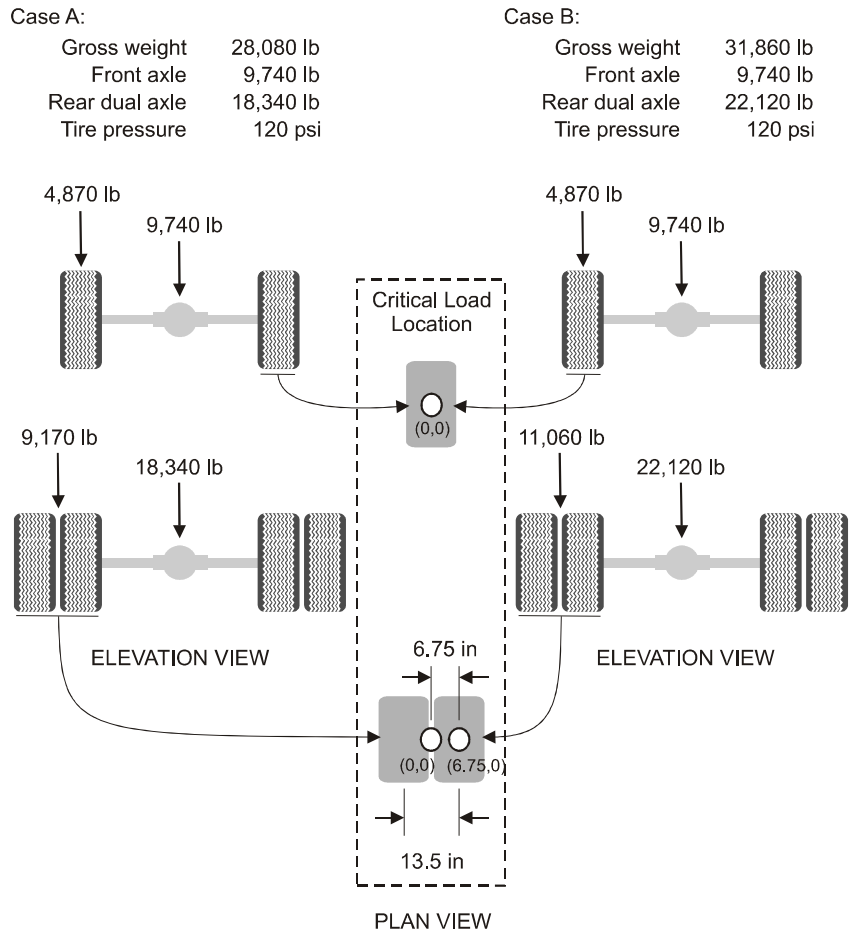
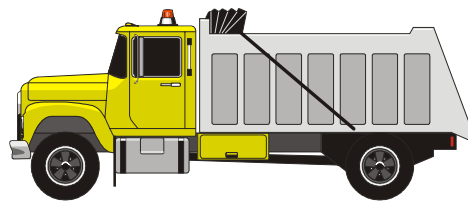


Figure 9. Dump Truck Loading Testing at Two Load Levels



Figure 10. Falling Weight Deflectometer Deflection Testing at Four Load Levels

Based on the FWD deflection testing, backcalculation was performed in two ways: on top of the FOSS and between the FOSS based on testing between the wheel paths. The FWD backcalculation results were used (1) in the determination of the stiffness of the pavements layers at and away from the FOSS locations and (2) as directed input in the MLE analysis to predict the strains at various load levels corresponding to single- and dual-axle DTLs and various FWD load levels.

RESULTS AND DISCUSSION

Predicted Theoretical and In-Situ Pavement Strain

Through the use of the MLE analysis program ELSYM5, pavement responses were calculated at four load levels, various depths, and critical pavement locations. The detailed results are presented in Appendix B.

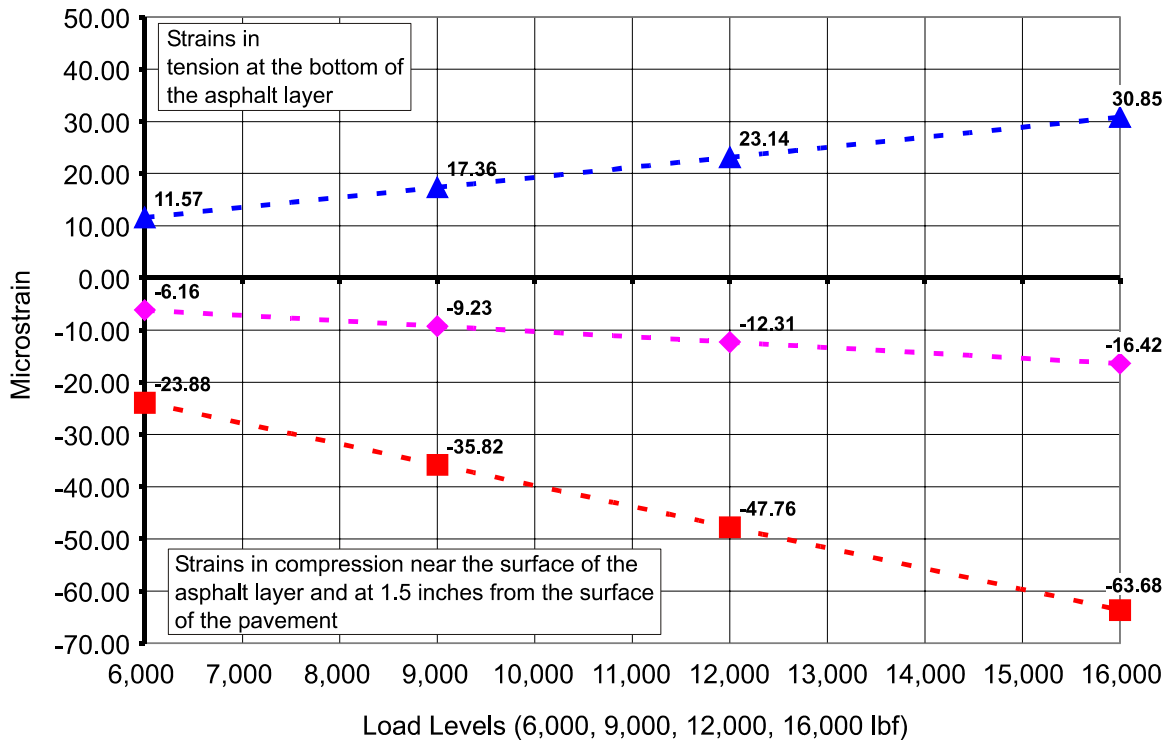
The pavement layers were modeled and approximated by the previously described four-layer pavement system (Figure 1). Table 5 shows the calculated theoretical strains at the four load levels at various pavement depths. As it can be seen from Figure 11, the relationship between the predicted strains and the load level was linear. This linear relationship was used to interpolate the strains under the surface layer 1.5 in from the top of the finished pavement. This relationship was also used to approximate the potential generated strains during construction (HMA delivery truck, paving operations, and roller operations).

Based on the results shown in Figure 11, the projected strains under the HMA delivery truck were estimated to be at least 50 fold in magnitude of the strains generated at typical truck loadings ranging between 30 and 45 microstrains in tension. This can be explained by the fact that the FOSS were unprotected under a thin layer of asphalt and the HMA covering them was not confined in the lateral direction. The high temperature generated from the installation process and the direct contact of the FOSS and the truck tires at this high temperature made the

Table 5. Calculated Microstrains at Critical Pavement Locations Under Load Plate

Location	Strain Type	0 in	0.1 in	9.4 in
SS-1 6,000 lb	EXX	-25.15	-23.88	11.57
	EYY	-25.15	-23.88	11.57
	EZZ	-18.35	-19.68	-26.81
SS-2 9,000 lb	EXX	-37.72	-35.82	17.36
	EYY	-37.72	-35.82	17.36
	EZZ	-27.52	-29.53	-40.21
SS-3 12,000 lb	EXX	-50.30	-47.76	23.14
	EYY	-50.30	-47.76	23.14
	EZZ	-36.70	-39.37	-53.61
SS-4 16,000 lb	EXX	-67.06	-63.68	30.85
	EYY	-67.06	-63.68	30.85
	EZZ	-48.93	-52.49	-71.48

EXX = Strains in the transverse direction; EYY=strains in the longitudinal direction; EZZ = strains in the vertical direction.. A negative sign is an indicator of compression.



▲ - Strain 9.5 in. Below Surface ◆ - Strain 1.5 in. Below Surface ■ - Pavement Surface Strain

Figure 11. ELSYM5 Calculated Strains at Different Pavement Depths and Different Load Levels

research team believe that strains 50 fold in magnitude of the theoretical calculated strains under FWD loading and/or DTL were reasonable.

The paving operation strains under high-temperature conditions were estimated to be higher by a factor of 1.5 than the strains generated during the HMA delivery operations. The

base mix sensors after the delivery of the HMA mixture and during the paving operations were subjected to high temperatures and loading generated by the paving operation itself under the paver hopper and the paver screed.

Finally, the roller-generated strains were estimated to be greater by a factor less than 1.5 times the paving operations strains as the mixture cooled down slightly and as the FOSS became more protected by the thickness of the base layer.

Table 6 shows projected strains based on theoretical MLE analysis predictions for the HMA delivery, paving, and compaction operations.

Strain values were expected to be within these ranges during the installation and the subsequent construction operations. The research team was concerned whether the FOSS would be able to monitor the high projected strains with a high degree of reliability. However, the FOSS were calibrated within the range of plus/minus 2,000 microstrains. The system can be designed and operated at a much wider range of plus/minus 20,000 microstrains as shown in Table 4.

Table 6. Projected Strains Based on Theoretical MLE Analysis Predictions

Operation Type	Projected Strains
HMA delivery truck	1,500-2,250 microstrains
Paving operations	2,250-3,375 microstrains
Compaction: Roller operation	3,375-5,062 microstrains

In-situ FOSS Measurements and Calibration

A typical response during the calibration procedure is shown in Figure 12. The FOSS response was linear between 500 and 2000 microstrains and between -500 and -2500 microstrains. However, the response from -500 to 500 microstrains was non-linear. Further, each sensor had a slightly different response to the applied displacement; thus each sensor was individually calibrated. Testing of five sensors indicated the mean was 0.45 microstrain with a standard deviation of 0.09 microstrain. Therefore, the sensitivity of the pavement strain sensors was better than 1 microstrain based on a conservative gap measurement resolution of 1 nm.

Although some nonlinearity in the FOSS response was observed during the development stage of this project, the research team decided it did not constitute a significant concern with the sensors designed for the field installation with their expected range of operation. During the manufacturing of the FOSS, two types of lines were used to fit the data: a linear trend line and a third-order polynomial function. This was done to understand the linearity of the data. Table 7 shows that the linear trend line demonstrates a very strong fit when compared to the third-order polynomial line. This also demonstrates the linear response of the FOSS during loading.

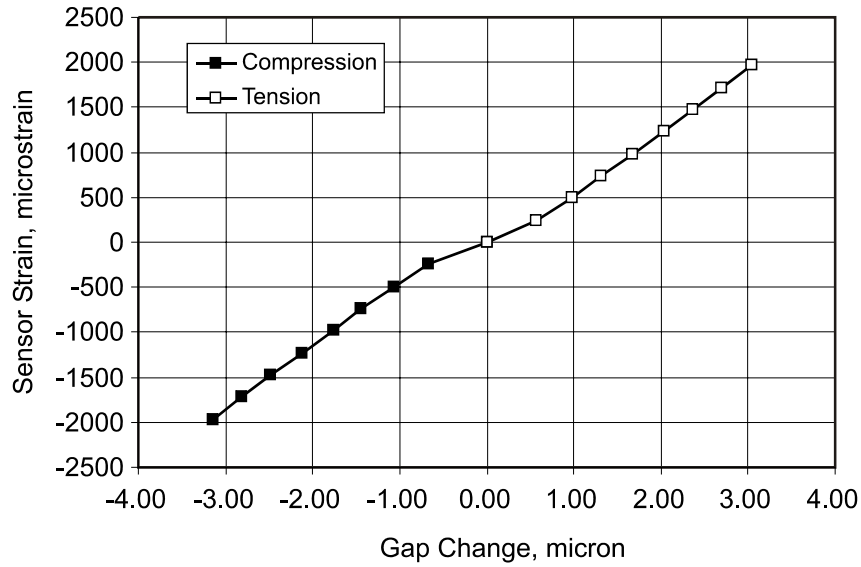


Figure 12. Example of Fiber-Optic Strain Sensor Calibration Curve

Table 7. Comparison of R^2 Values Based on Third-Order Polynomial and Simple Linear Fit

Sensor	R^2 Linear	R^2 3rd Order Polynomial	Difference in R^2 Fit Values
1SMR	0.9993	0.9999	0.0006
1SML	0.9938	0.9991	0.0053
2SMR	0.9995	0.9996	0.0001
2SML	0.9954	0.9989	0.0035
3SMR	0.9987	0.9993	0.0006
3SML	0.9992	0.9998	0.0006
4SMR	0.9966	0.9994	0.0028
4SML	0.9991	0.9994	0.0003
5SMR	0.9999	0.9999	0.0000
5SML	1.0000	1.0000	0.0000
1BMR	0.9942	0.9979	0.0037
1BML	0.9977	0.9992	0.0015
2BMR	0.9983	0.9988	0.0005
2BML	0.9986	0.9997	0.0011
3BMR	0.9992	0.9999	0.0007
3BML	0.9995	0.9998	0.0003
4BMR	0.9962	0.9993	0.0031
4BML	0.9980	0.9998	0.0018
5BMR	0.9823	0.9972	0.0149
5BML	0.9990	0.9998	0.0008
Average Difference			0.0021
Standard Deviation			0.0034

In-situ Strain Measurements Under HMA Delivery Truck, Paver, and Roller Loadings

HMA Delivery Truck and Paver Loadings

Strain measurements were made as the base mix was being placed. Table 8 is a guide to the paving operations and highlights the changes in strain shown in Figure 13.

Figure 13 shows the in-situ strain measurement monitored under the paving operations. Figure 13A (time from 0 to about 800 sec) shows the entire paving operations starting from the HMA delivery to the paver hopper, with direct loading on top of the unprotected FOSS. Figure 13B (time from 210 to about 235 sec) is a subset of Figure 13A and shows the back and front axle of the dump truck feeding the HMA mixture to the paver hopper. In-situ strain measurements were approximately 3100 microstrains under the rear axle of the HMA delivery truck, 2600 microstrains under the front axle of the HMA delivery truck, and about 4800 microstrains under the paver loading.

As can be seen, the strains were close to the predicted strains using MLE analysis. The observed strains were higher than the predicted strains. This was not a surprise, since the MLE analysis was conducted prior to construction and was only an estimate, based on approximate loading conditions. Construction loading (truck loading and paver loading) will vary by the type of field equipment used.

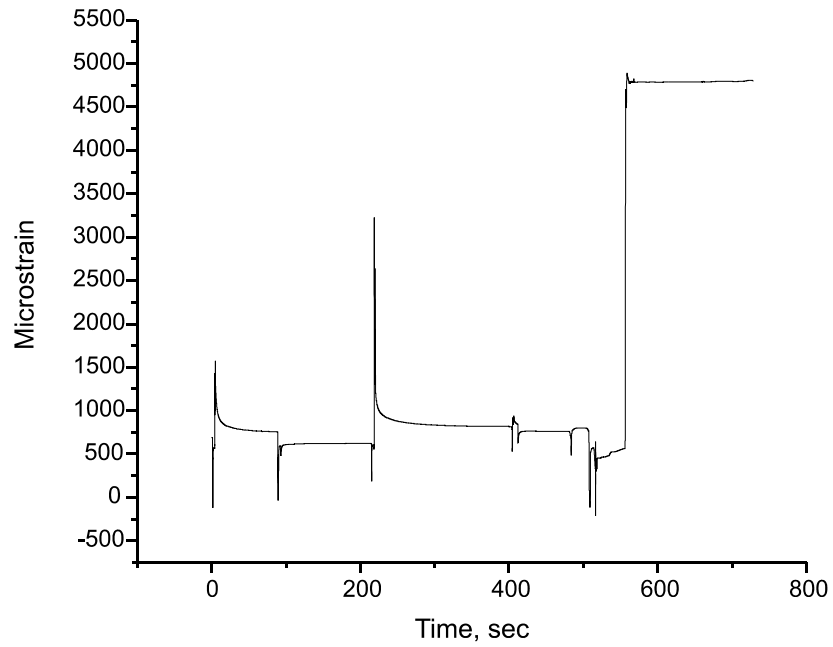
The measured FOSS strains were affected by the temperature of the HMA pavement layer, the traffic loading, and the traffic speed. The FOSS and thermocouples were placed under a thin layer of asphalt right before the paving operation began. It was clear from the temperature data that the thin layer of asphalt had cooled (as expected) and was then reheated by the asphalt during the paving operation. As shown in Figure 14, after the paver had passed over the sensor but before the roller operations, the strain and the temperature increased in the base mix. This figure also shows an increase of 5 microstrains per degree (approximately 3 microstrains per degree Fahrenheit) in a 10-min period of time.

Table 8. Events Measured by Fiber-Optic Strain Sensors During Paving Operations

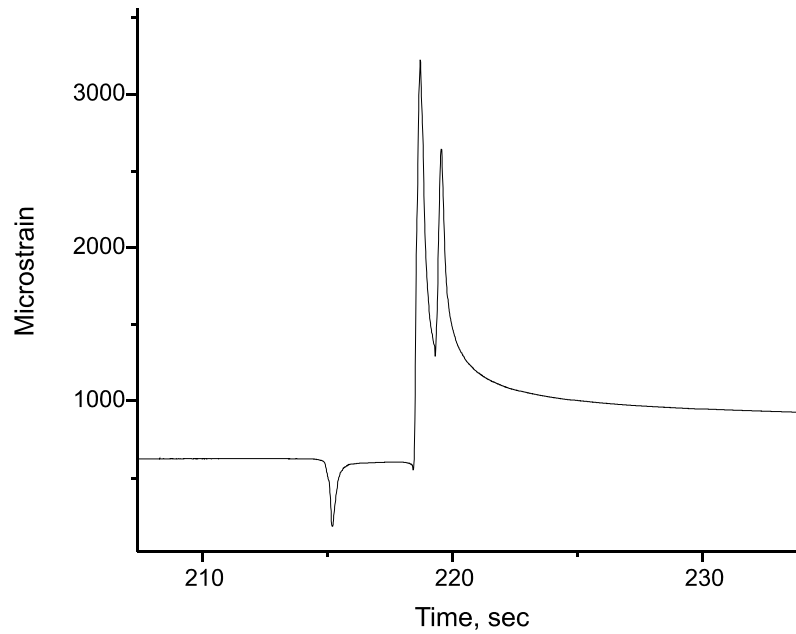
Vehicle	Direction	Time, sec
Dump truck	Forward	1.5
Dump truck	Reverse	90
Dump truck	Forward	215
Dump truck	Reverse	404
Dump truck	Forward	486
Paver	Forward	555

Compaction Loading

Similarly, during the compaction of the base mixture, the response of the FOSS was also monitored as the roller moved forward and backward parallel with the longitudinal direction of the pavement cross section and as the roller moved transversely between the right and the left wheel paths. The process is described in Table 9, and the results are shown in Figure 15.



(A)



(B)

Figure 13. Strain Measurements Recorded During Paving Operation. (A) Entire timeline up to paver crossing over sensor. (B) Zoom in on forward movement of dump truck loaded with asphalt; sensor unprotected; shovel full of asphalt cover.

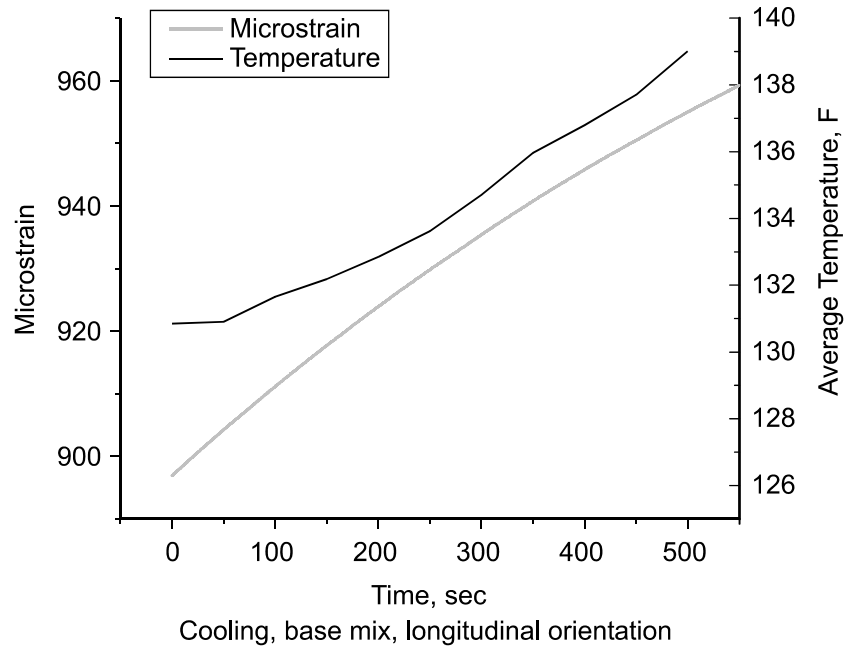
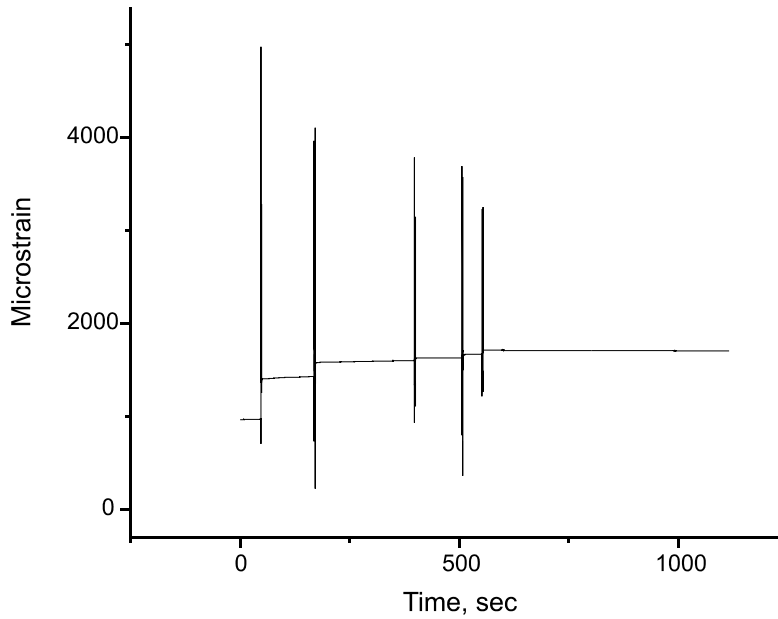


Figure 14. Strain and Temperature Change During Cooling (After Paving But Prior to Rolling) in Base Mix and Longitudinal Sensor Orientation

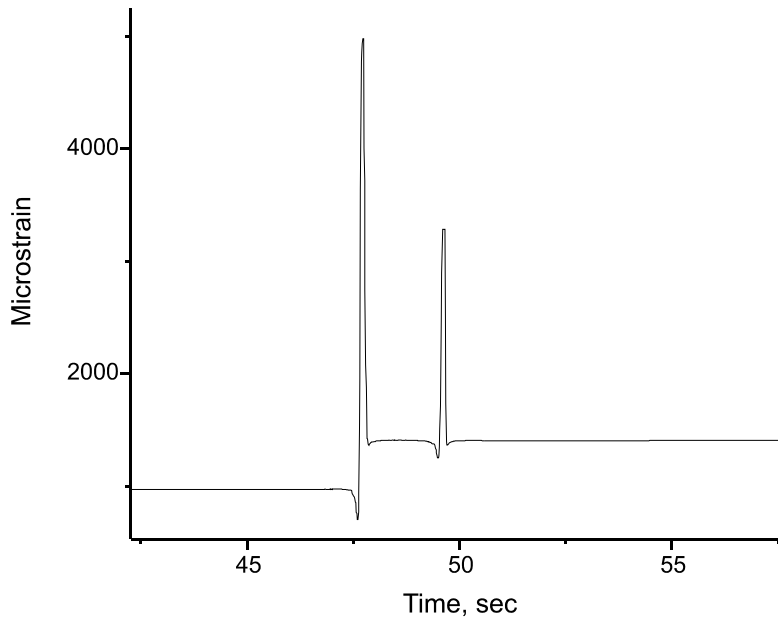
Table 9. Roller Event Resulting in Strain Indication During Compaction Process

Direction	Wheel Path	Time, sec
Forward	Left	57
Backward	Left	180
Forward	Right	240
Backward	Right	352
Forward	Left	408
Backward	Left	516
Forward	Left	562
Backward	Right	674
Forward	Right	728
Backward	Right	840
Forward	Left	888
Backward	Seam	1,002
Forward	Seam	1,044

In-situ strains were measured between approximately 3000 and 5000 microstrains as the roller moved forward and backward. The predicted strains using MLE analysis ranged between 3375 and 5062 microstrains, as presented in Table 6. As can be seen, the predicted MLE analysis strains were comparable to the measured in-situ strains. This is not surprising since the FOSS became more protected because of the thick HMA base.



(A)



(B)

Figure 15. Strain Measurements Recorded During Rolling Operation. (A) Entire timeline during rolling. (B) Zoom in on forward movement of roller.

Strain Measurement Under Dump Truck and FWD Loadings

Upon completing the construction process, it was determined that 80% of the FOSS at the bottom of the surface mix and 50% of the FOSS at the bottom of the base mix survived. The reason for the higher failure rate at the base layer was because some of the sensor leads were

accidentally severed during shoulder construction, whereas this was avoided during the placement of the surface FOSS. Figure 16 shows the orientation and operational condition of each FOSS following the placement of the base mix and surface mix. After the pavement was constructed, a DTL at variable speeds and loadings and an FWD loading experiment were conducted in the summer and fall of 2004.

	<--- North (Bridge)		<u>Surface Mix</u>		South --->
Station # -->	<u>1</u>	<u>2</u>	<u>3</u>	<u>4</u>	<u>5</u>
Driver Wheel Path	Bad -L	Good -T	Good -L	Good -T	Good -L
Passenger Wheel Path	Bad -T	Good -L	Good -T	Good -L	Good -T
Shoulder					

-L for longitudinal -T for transverse

(A)

	<--- North (Bridge)		<u>Base Mix</u>		South --->
Station # -->	<u>1</u>	<u>2</u>	<u>3</u>	<u>4</u>	<u>5</u>
Driver Wheel Path	Bad -L	Good -T	Good -L	Bad -T	Bad -L
Passenger Wheel Path	Good -T	Good -L	Bad -T	Good -L	Bad -T
Shoulder					

-L for longitudinal -T for transverse

(B)

Figure 16. Orientation and Operational Condition of Sensors (*good* meaning sensor works and *bad* meaning sensor failed). Following paving operation for (A) surface mix course and (B) base mix course.

Dump Truck Loading

Two DTLs were used, at variable speeds. The first was performed near “static loading conditions” at 1 mph, and the second was performed at 45 mph, which is a typical speed under real truck traffic loading conditions. The axles were weighted each time; the results for the higher weight truck (gross weight 31,860 lb) were compared to strains produced at the same loads using a MLE analysis.

The MLE analysis were performed twice, the first time using the theoretical pavement layer moduli presented in Table 3, and the second time using the in-situ layer moduli based on the FWD deflection data and the backcalculated in-situ layer moduli.

Measurements at the slower travel rate (1 mph) exhibited reproducible strain responses. Figure 17 shows the strain response of the FOSS to forward and reverse motion of the truck. These responses, gathered at two times (from 35 to 45 sec and 85 to 95 sec), are mirror images for FOSS embedded beneath the surface and the base mixtures. For a pair of measured strain response, the FOSS below the surface mix indicate compression (negative strain values) while simultaneously the FOSS below the base mix indicate tension (positive strain value), similar to what was found in the theoretical pavement response analysis. Table 10 shows the peak measured strain values for each axle and direction.

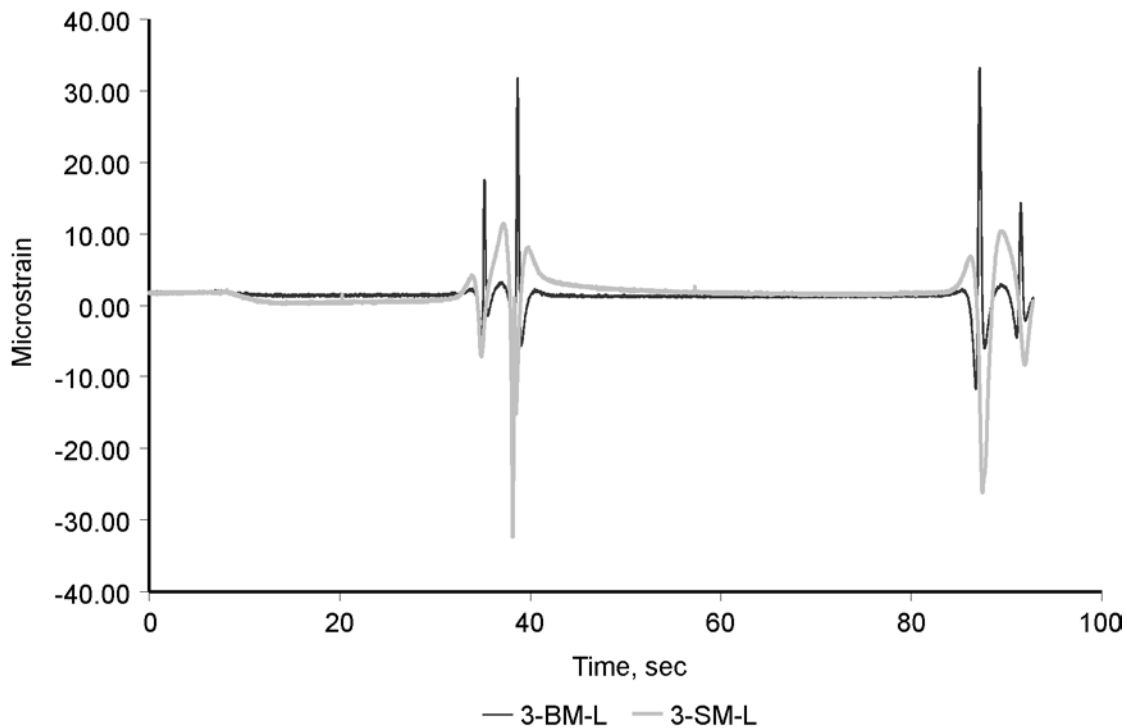


Figure 17. Response of Surface and Base Mix Sensors Subjected to Dump Truck Moving Forward at Approximately 1 mph and Then in Reverse at Approximately 1 mph. Gross weight 31,860 lb (rear axle 22,120 lb).

Table 10. Maximum Microstrains as Result of Dump Truck moving at Approximately 1 mph

Sensor	Forward Motion		Reverse Motion	
	Front Axle	Rear Axle	Front Axle	Rear Axle
Surface mix	-7.0	-32.2	-8.3	-26.0
Base mix	17.6	31.8	14.4	33.3

Gross weight 31,860 lb (rear axle 22,120 lb).

Further, the measured strain response is consistently reproduced among three consecutive truck loadings as shown in Figure 18. The variability of the measured strains among the three forward and backward loadings is consistent and limited in magnitude, as shown in Figure 18. The front axle strains are ranging between approximately 12 and 18 microstrains, and the back axle strains are ranging between approximately 29 and 33 microstrains. This is consistent with the MLE analysis results at 9,000 and 12,000 lb, which corresponds to a surface pressure of approximately 82 and 100 psi, respectively.

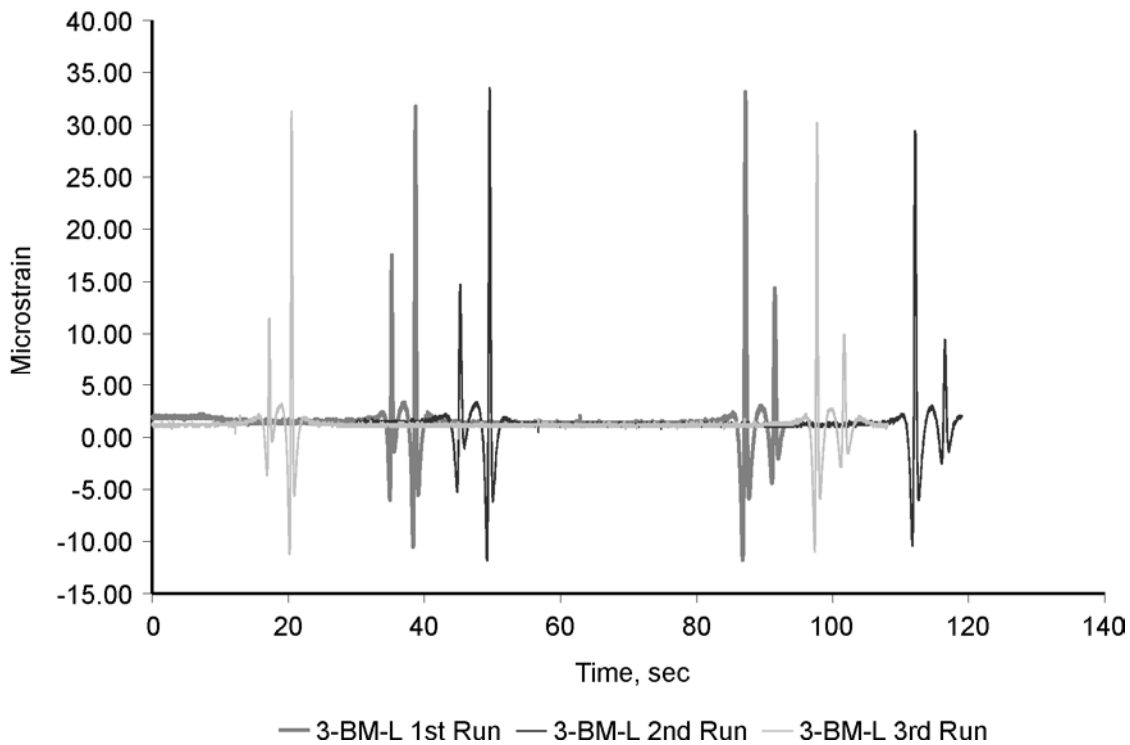


Figure 18. Response of Single Base Mix Sensor Repeatedly Subjected to Dump Truck Moving Forward at Approximately 1 mph and Then in Reverse at Approximately 1 mph. Gross weight 31,860 lb (rear axle 22,120 lb).

Table 11. Maximum Microstrains in Base Mix as Result of Dump Truck Moving at Approximately 1 mph

Run	Forward Motion		Reverse Motion		Average	
	Front Axle	Rear Axle	Front Axle	Rear Axle	Front Axle	Rear Axle
First	17.6	31.8	14.4	33.1	12.8	31.5
Second	14.4	33.4	9.4	29.4		
Third	11.5	31.3	9.4	30.1		

Gross weight 31,860 lb (rear axle 22,120 lb).

The FOSS measurements using a loaded truck at two speeds indicated that the FOSS were responding under nearly static (at 1 mph) and dynamic (at 45 mph) loading conditions. However, the resolution of measurements at 45 mph was not as clear as measurements at 1 mph, shown in Figures 19 and 20. It is evident in Figure 20 that the FiberScan 2000 device was not able to measure the peak response clearly at the higher speed, i.e., reduced rate of loadings.

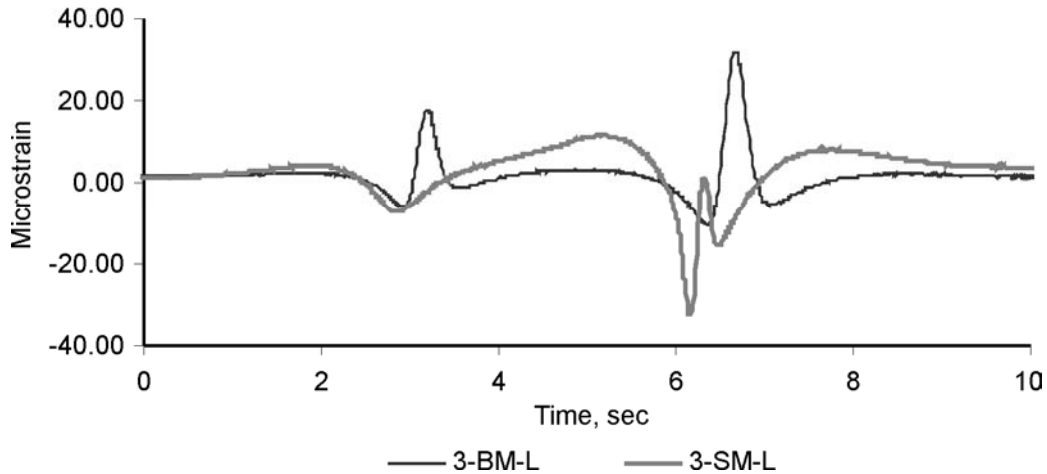


Figure 19. Sensor Measurement Using Loaded Dump Truck Traveling Approximately 1 mph. Gross weight 31,860 lb (rear axle 22,120 lb).

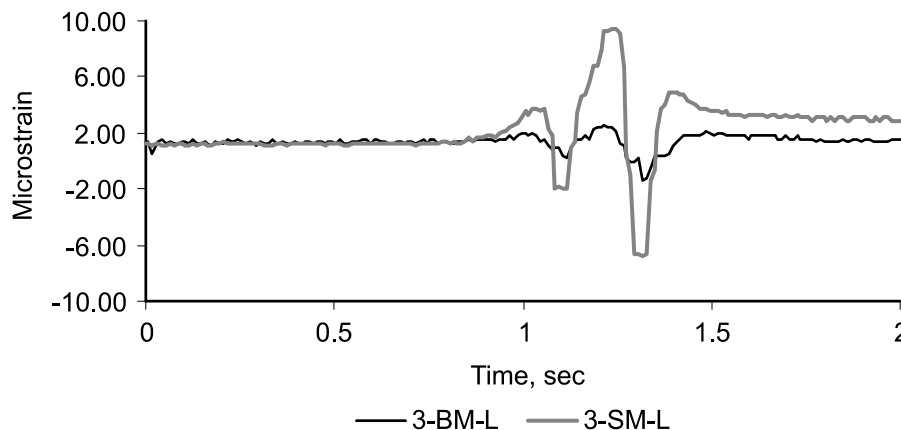


Figure 20. Sensor Measurement Using Loaded Dump Truck Traveling Approximately 45 mph. Gross weight 31860 lb (rear axle 22,120 lb).

The base mix FOSS measurements shown in Figures 19 and 20 were superimposed to produce Figure 21. Figure 21 demonstrates the loss of resolution at higher speeds. It is clear that the strain response of each axle is visible at lower speeds, but at higher speeds, Figure 21 would indicate the strain is almost nonexistent when the FiberScan 2000 was used because the peaks are ill-defined.

In an attempt to obtain clearly defined peaks, a six-axle truck loading experiment was conducted during the summer of 2005. Only the results relevant to better peak resolution and measurements at higher speeds are presented here.

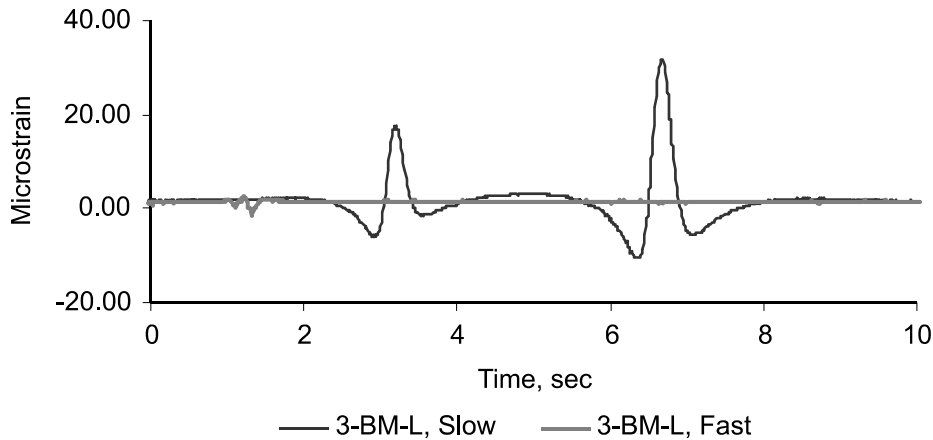


Figure 21. Sensor Measurement Using Loaded Dump Truck Traveling 1 and 45 mph. Gross weight 31,860 lb (rear axle 22,120 lb).

In this experiment, a FiberPro2 device was used for strain measurements, and the loss in resolution was no longer an issue. Figures 22 and 23 show the response of a FOSS as measured by the FiberPro2 device at slower (35 mph) and faster (55 mph) speeds. It is clear in Figure 22 that each axle is inducing a response from the FOSS. Further, as the load configuration is changed and the rear three axles begin to carry a greater load, the response of the FOSS to these axles also increases. In Figure 22, the strain created by the front steering axle increases slightly with the increase in load, but the strains with the other axles increase considerably as the load is increased. This was expected since the load placed on this type of tractor-trailer unit is situated between the two tractor axles and the three trailer axles. Clearly, the measurement made using the FiberPro2 unit exhibits greater clarity and peak clipping is no longer evident.

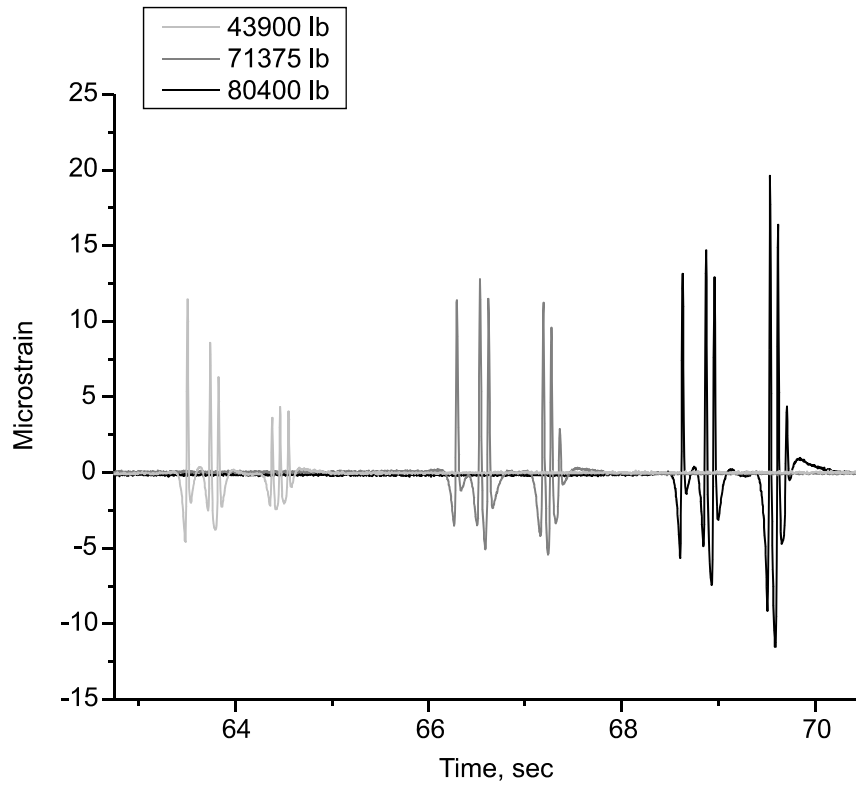
In Figure 23, the same six-axle tractor-trailer was used with the same load conditions, but the rate of travel was increased from 35 to 55 mph. The peaks attributable to the various loads on each axle can still be distinguished, but the maximum strain values are lower. The strain response of the pavement is consistent with what is expected from this type of loading.

As expected, the temperature in the base mix remained much more constant as compared to the temperature below the surface mix. Figure 24 shows that as the air temperature began to increase, so did the temperature of the surface mix. As a point of reference, the maximum, minimum, and average air temperatures for each test date are provided in Table 12.

FWD Loading

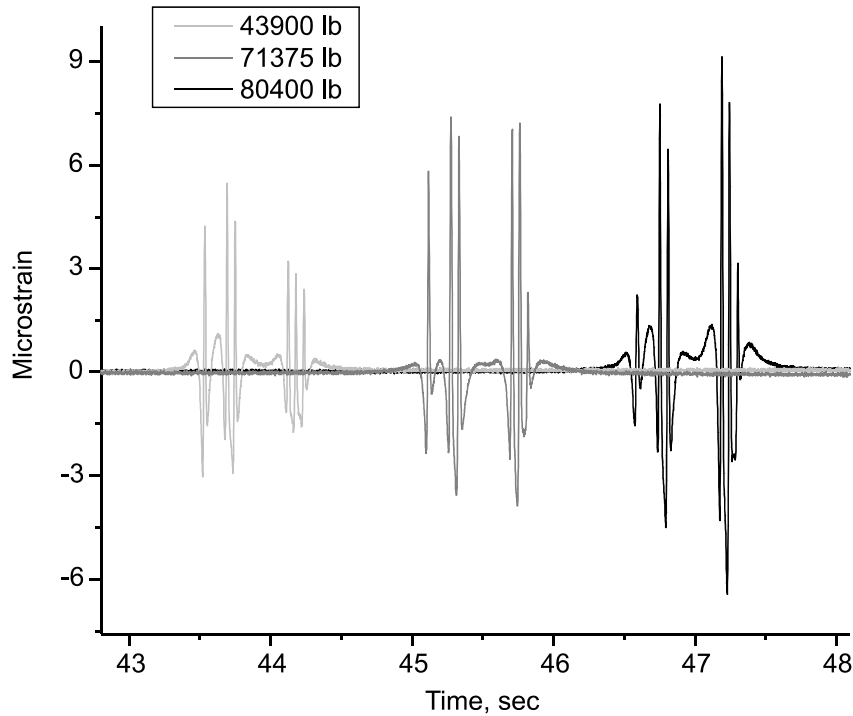
FWD deflection testing, after construction and dump truck loading, was performed on top of the FOSS on the right and left wheel paths. It was hypothesized that the backcalculated pavement layer moduli would be similar for both wheel paths.

Further, FWD deflection testing was performed longitudinally up and down along the longitudinal direction on top of and away from the FOSS. It was hypothesized that the backcalculated pavement layer moduli (stiffness) results on top of and away from the FOSS should be similar to conclude that the FOSS installation had no significant impact on the stiffness of the pavement layers.



Sensor 4: Base Mix Right Side-35 mph - Transverse

Figure 22. Response of Sensor in Base Mix to Six-Axle Vehicle Traveling 35 mph with Various Gross-Vehicular Weights



Sensor 3: Base Mix Left Side-55 mph - Transverse

Figure 23. Response of Sensor in Base Mix to Six-Axle Vehicle Traveling 55 mph with Various Gross-Vehicular Weights

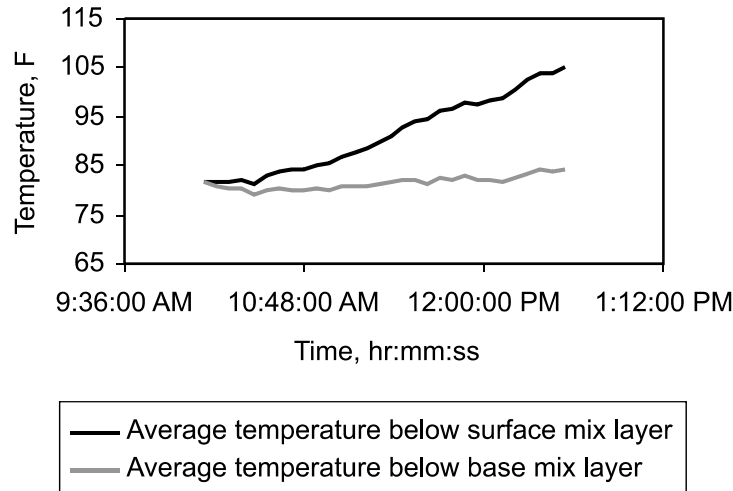


Figure 24. Comparison of Temperature Below Surface Mix and Below Base Mix Layers on September 10, 2004

Table 12. Air Temperature Data for Dump Truck and Falling Weight Deflectometer Tests

Test Description (Date)	Minimum Temperature, F	Maximum Temperature, F	Average Temperature, F
Dump truck, 31,860 lb gross (09/10/04)	56	80	68
FWD (09/21/04)	43	79	61
Dump truck, 28,080 lb gross (11/01/04)	50	79	65

This hypothesis was further evaluated during the summer of 2005. FWD deflection data were obtained on top of the FOSS and between the wheel paths approximately 3 feet from the FOSS embedded in the left or right wheel paths. Only the results relevant to pavement stiffness are presented in this report.

The FWD backcalculation results from the 2004 construction season are shown in Appendix B. The MLE analysis summaries are also presented in Appendix B. Table 13 shows the strains observed at the first FOSS and the air and surface temperature corresponding to strain calculated at this sensor location based on FWD deflection testing. The table also shows the backcalculated results used in ELSYM5 to generate the strains under the asphalt pavement.

The backcalculated results were used to produce MLE strains, and the MLE strains were compared to the measured strains under DTL (23 to 24 microstrains). The in-situ measured strains were very similar to the strains calculated in the MLE analysis .

As a result of the FWD loading experiment and as shown in Appendix B, the backcalculated results for the right and left wheel paths were not statistically different but were greatly influenced by the increased air temperature during FWD testing. In addition, the backcalculated results on top of and away from the FOSS were not statistically different. In addition, there was a strong and good relationship between the asphalt stiffness and the measured air and surface temperatures. These values are typically used to calculate the pavement temperatures and are shown in Figures 25 and 26, respectively.

Table 13. Strains Observed at First Fiber-Optic Strain Sensor Location

Strain Type	Strains Under Load Plate									
	0 in	0.1 in	9.4 in	12.4 in	12.6 in	19.4 in	19.6 in	25.4 in	25.6 in	37.5 in
EXX (1)	-41.03	-38.90	22.83	18.39	18.23	24.09	24.24	23.40	23.35	12.53
EYY (1)	-41.03	-38.90	22.83	18.39	18.23	24.09	24.24	23.40	23.25	12.53
EZZ (1)	-30.55	-32.79	-47.26	-44.55	-43.22	-21.96	-49.10	-38.32	-55.92	-30.95
EXX (2)	-41.58	-39.44	23.87	19.10	18.91	24.31	24.46	23.76	23.72	12.70
EYY (2)	-41.58	-39.44	23.87	19.10	18.91	24.31	24.46	23.76	23.72	12.70
EZZ (2)	-29.79	-32.05	-47.97	-46.38	-45.00	-22.72	-49.31	-38.64	-56.73	-31.35
Location	Sensor No.	Test No.	E1	E2	E3	E4	Load	Pavement Surface Temp. (F)	Air Temp. (F)	
RWP 0.000+0.0	1	1	857,353.00	464,829.00	135,540.00	53,113.60	11,282.96	81.90	63.60	
RWP AVG 0.000	1	All (3)	862,324.40	442,373.10	137,575.30	52,930.90	11,323.06	83.57	63.70	

EXX = strains in transverse direction; EYY = strains in longitudinal direction; EZZ = strains in vertical direction; RWP = right wheel path. A negative sign is an indicator of compression.

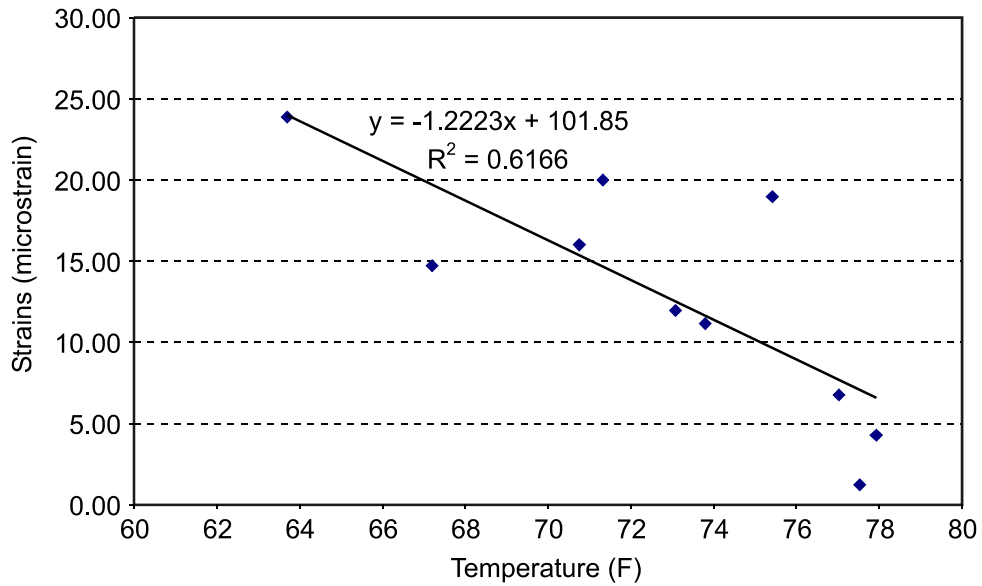


Figure 25. Air Temperatures Versus Predicted Microstrains

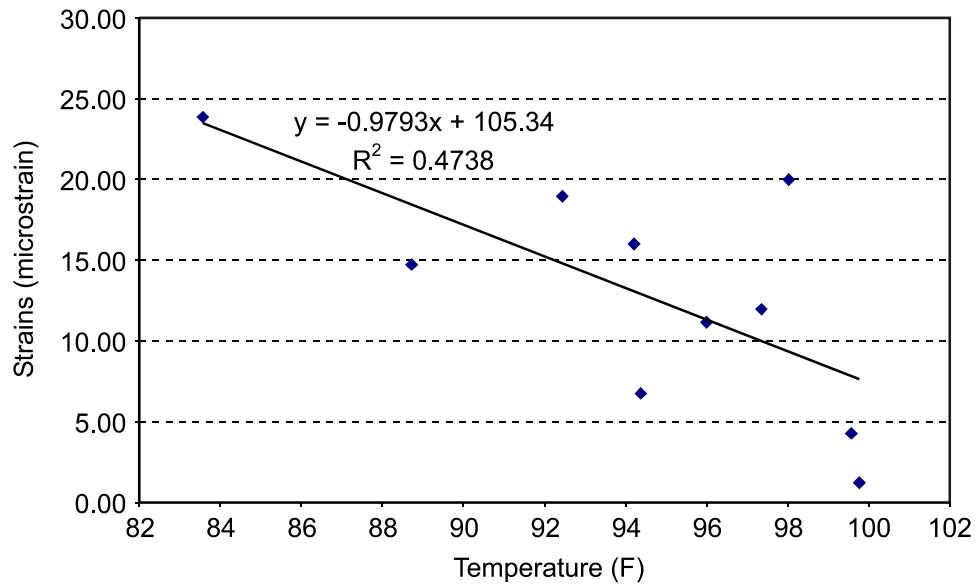


Figure 26. Surface Temperatures Versus Predicted Microstrains

Future FOSS Testing

Long-term in-situ performance is a major objective of this study. Annual dynamic loading experiments are planned to validate and monitor the FOSS strains under this pavement section. Dynamic truck loading at variable speeds and loading experiments followed by FWD deflection testing at various load levels were conducted during the summer of 2005.

To measure the sensitivity of FOSS to strain changes under truck loadings, the FOSS were trafficked by a six-axle truck at three load levels and under different traffic speeds. The results of the FiberPro2 and the FiberScan2000 comparisons were presented in this report. Further analysis of the strain sensitivity to various loads and speeds will be performed later. FWD deflection testing was carried out at two locations: on top of the FOSS embedded in the pavement layers and between the wheel paths. The backcalculation was performed for each location to determine the effect of these FOSS on the backcalculated moduli (stiffness) of the pavement layers. The moduli were used in the MLE analysis program ELSYM5 to estimate the pavement responses (stresses, strains, and deflections) under the FWD loads. These responses, especially the strains, were later compared to the measured fiber optics strains under the same FWD loads. A similar FWD loading experiment is planned for the fall of 2006; however, FWD dynamic data (load histories) will also be collected. Three-dimensional (3D) finite element modeling and analysis techniques will be used to validate further the FOSS results generated under dynamic loads.

A small laboratory study was also conducted to monitor the strain under axial loading. The FOSS were embedded in 4-inch-thick asphalt beams, and strains were measured as the beams were statically and dynamically loaded. The strains were compared to those obtained using MLE analysis and will be compared to those obtained from 3D-finite element modeling techniques. Asphalt beams were constructed using different HMA mixtures.

CONCLUSIONS

- Placing an EFPI FOSS during normal asphalt paving operations is feasible.
- The FiberScan2000 signal conditioning unit is adequate for measuring the strain near static conditions or at a slow loading rate.
- The FiberPro2 signal conditioning unit should be used for making dynamic measurements at highway speeds.
- FWD deflection data and analysis at various drop levels and the subsequent strain calculations indicate that the observed fiber-optics strain measurements are very close to predicted theoretical or backcalculated strains.
- Based on FWD loadings, the observed fiber-optic strain measurements under truck loading are similar to predicted theoretical strains and backcalculated strains.
- The embedded EFPI FOSS is sensitive enough to capture the influence of an adult human jumping on the completed pavement surface above the base mix sensor.
- The embedded EFPI FOSS is able to capture the influence of each axle of a six-axle tractor-trailer moving at 55 mph.
- MLE analysis adequately predicts pavement strains at critical pavement locations.

RECOMMENDATIONS

1. The Virginia Transportation Research Council (VTRC) and VDOT's Materials Division should use FOSS for further evaluation in future pavement installations using different pavement types and layers.
2. VTRC and VDOT's Materials Division should use MLE analysis to predict pavement strains at critical pavement locations when designing or evaluating pavement structures.
3. VTRC should use FWD deflection testing to evaluate the FOSS that will be placed at other pavement sites. Dynamic (load history) and peak deflection data are necessary for future evaluation of FOSS.
4. VTRC should use three-dimensional finite element modeling for further evaluation of the MLE analysis presented in this research study.

BENEFITS AND COSTS ASSESSMENT

Premature pavement failures can result from designing and constructing asphalt pavements that are too thin. On the other hand, conservative asphalt pavement designs result in thick asphalt pavements with higher construction costs. Understanding the behavior of asphalt pavement under repeated traffic (dynamic) loads can result in an optimized asphalt pavement design, thus reducing the rehabilitation costs associated with premature failures or the higher costs associated with conservative asphalt pavement designs.

For example, pavement management data show that more than 90% of Virginia's roadways are constructed and/or rehabilitated using asphalt pavements. Reducing the pavement thickness by 0.5 inch can save an estimated \$15,000 per lane mile in materials cost alone. Over-designing can quickly increase the materials cost for VDOT during paving. If the pavement is under-designed, premature failure of the flexible pavement system could result, which would lead to maintenance at an earlier date than expected.

It is anticipated that the results of this research study will provide pavement engineers with a better understanding of the effects of dynamic loading (repeated traffic loads) on a pavement structure. This information will be useful in validating future designs. It will also provide a novel technique for evaluating new pavements in the field with minimal disruption to the paving process.

ACKNOWLEDGMENTS

The research team acknowledges the following individuals for their valuable contributions to the successful completion of this study: Charles Babish, Don French, Cesar Apusen, Eileen Aiken, Troy Deeds, Thomas Hall III, Mike Grishaw, David Thacker, Kevin Cooper, Jason Chevalier, Laurence Platt, Dan Blevins, Nate Brown, and Tom Wavering. The research team also acknowledges Michael Sprinkel and Kevin McGhee for their valuable

comments and suggestions during the review process of this report. The research team also acknowledges Linda Evans for her valuable editorial efforts that led to the finalization of this report. The research team also acknowledges Derek Guthrie for his assistance in running the MLE analysis program ELSYM5. In addition, the research team acknowledges the Virginia Transportation Research Council for providing the necessary funding of this research project.

REFERENCES

- Al-Qadi, I. L., Loulizi, A., Elseifi, M., and Lahouar, S. The Virginia Smart Road: The Impact of Pavement Instrumentation on Understanding Pavement Performance. *The Journal of the Association of Asphalt Paving Technologists*, Vol. 73, 2004, pp. 427-466.
- de Vries, M.J., Murphy, K.A., Poland, S.H., Arya, V., and Claus, R.O. *Optical Fiber Sensors for Civil Structure Applications: A Comparative Evaluation*. Paper presented at the First World Conference on Structural Control, Los Angeles, August 3-5, 1994.
- de Vries, M.J., Poland, S.H., Grace, J.L., Arya, V., Murphy, K.A., and Claus, R. Optical Fiber Sensors for Advanced Civil Structures. In *Proceedings of the 11th ASCE Engineering Mechanics Conference*. American Society of Civil Engineers, New York, 1996.
- Federal Highway Administration. *Pavement Analysis and Design Checks. Participant's Manual*. FHWA-HI-95-021. Washington, DC, 1995.
- Huang, Y.H. *Pavement Analysis and Design*. Prentice Hall, Inc., Englewood Cliffs, NJ, 1993.
- Loulizi, A., Al-Qadi, I. L. Lahouar, S., and Freeman, T.E. Data Collection and Management of the Instrumented Smart Road Flexible Pavement Sections. In *Transportation Research Record 1769*. Transportation Research Board, Washington, DC, 2002, pp. 142-151.
- Masri, S.F., Agbabian, M.S., Abdel-Ghaffar, A.M., Higazy, M., Claus, R.O., and de Vries, M.J. Experimental Study of Embedded Fiber-Optic Strain Gauges in Concrete Structures. *Journal of Engineering Mechanics*, Vol. 120, No. 8, 1994, pp. 1696-1717.
- Safaai-Jazi, A., Ardekani, S.A., and Mehdikhani, M. *A Low-Cost Fiber Optic Weigh-in-Motion Sensor*. SHRP 90-002. Strategic Highway Research Program, Washington, DC, 1990.
- Sharp, S.R., Cooper, K.R., Clemeña, G.G., and Elfino, M.K. Fiber-Optic Based Strain Sensor for Asphalt Pavement. Paper presented at the 84th Annual Meeting of the Transportation Research Board (on CD of 2005 Annual Meeting). Transportation Research Board, Washington, DC, 2005.
- Thompson, M.R., Barenberg, E.J., Carpenter, S.H., Darter, M.I., and Dempsey, B.J. *Calibrated Mechanistic Structural Analysis Procedures for Pavements*. NCHRP 1-26. Transportation Research Board, Washington, DC, 1989.

- Uddin, W. Application of 3D Finite Element Dynamic Analysis for Pavement Evaluation. In *Proceedings of the First National Symposium Finite Element for Pavement Analysis and Design*, West Virginia, November 1998, pp. 95-109.
- Uddin, W. Simulation of Falling Weight Deflectometer for In-Situ Material Characterization of Highway and Airport Pavements. Proceedings of the 6th International LS-DYNA Users Conference Simulation 2000. Dearborn, MI, April 2000.
- Uddin, W., and Godiwalla, A. Finite Element Simulation of Nondestructive Testing for Pavement Structural Evaluation, American Society of Civil Engineers. In *Proceedings of the 25th International Air Transportation Conference*, Austin, TX, June 1998.
- Uddin, W., Momm, H., and Garza, S. Application of the PEDD Methodology of Modulus Backcalculation for TRB Nonlinear Pavement Analysis Project. CD Proceedings, Annual Meeting of the Transportation Research Board, National Research Council, Washington, DC, January 2003.
- Ullidtz, P. Modeling Flexible Pavement Response and Performance. Polyteknisk Forlag, Lyngby, Denmark, 1998.

APPENDIX A: SENSOR SPECIFICATIONS

SENSOR

Operational

Strain

- Range
 - Min. 50 microstrains
 - Max. 350 microstrains
- Accuracy, $\pm 1\%$
- Resolution, 1 microstrain
- Temperature sensitivity, 1 microstrain/ $^{\circ}\text{C}$ (0.6 microstrain/ $^{\circ}\text{F}$)

Operating Temperature

- Min. 5 $^{\circ}\text{F}$
- Max. 150 $^{\circ}\text{F}$

Mechanical

- Under wheel path
 - Min. 10 psi
 - Max. 150 psi
- Point load (assume total load applied over a $\frac{3}{4}$ -inch x $\frac{3}{4}$ -inch stone face): Max. 10,000 psi

Compliance/Stiffness

- 10,000 MPa at 50 $^{\circ}\text{F}$
- 1,000 MPa at 104 $^{\circ}\text{F}$

Dimensions (L x W x H): H < 2 in

Environmental (Chemical) Resistance

- Asphaltenes
- Naphtha
- Kerosene
- Mineral spirits
- Water
- Surfactants

Installation

Temperature: Max. 375 $^{\circ}\text{F}$

Mechanical

- Under wheel path
 - Min. 10 psi
 - Max. 150 psi
- Point load (assume total load applied over a $\frac{3}{4}$ -inch x $\frac{3}{4}$ -inch stone face): Max. 10,000 psi

Environmental (Chemical) Resistance

- Asphaltenes
- Naphtha
- Kerosene
- Mineral spirits
- Surfactants

SENSOR LEAD

Operational

Temperature

- Min. 5 °F
- Max. 150 °F

Mechanical

- Under wheel path
 - Min. 10 psi
 - Max. 150 psi
- Point load (assume total load applied over a 3/4-inch x 3/4-inch stone face): Max. 10,000 psi

Compliance/Stiffness

- 10,000 MPa at 50 °F
- 1,000 MPa at 104 °F

Environmental (Chemical) Resistance

- Asphaltenes
- Naphtha
- Kerosene
- Mineral spirits
- Water
- Surfactants

Installation

Temperature: Max. 375°F

Mechanical

- Under wheel path
 - Min. 10 psi
 - Max. 150 psi
- Point load (assume total load applied over a 3/4-inch x 3/4-inch stone face): Max. 10,000 psi

Environmental (Chemical) Resistance

- Asphaltene
- Naphtha
- Kerosene
- Mineral spirits
- Surfactants

APPENDIX B: MLE ANALYSIS PROGRAM ELSYM5 RESULTS

Table B1. ELSYM5 Input and FWD Backcalculated Data

Location	Sensor Number	Test Number	E1	E2	E3	E4	Load	Pavement Surface Temp. (F)	Air Temp. (F)
LWP 0.028+0.0	4	1	351,699.30	1,008,175.00	145,781.30	43,986.80	10,967.62	101.50	78.90
LWP 0.009-3.2	2	6	431,733.30	489,568.20	81,559.90	25,064.70	11,045.08	89.90	75.10
LWP AVG 0.000	1	All (1)	409,556.50	740,956.70	99,639.74	58,180.10	11,062.40	96.00	73.80
LWP AVG 0.009	2	All (6)	423,109.40	503,199.60	78,338.60	25,859.58	11,045.08	92.44	75.42
LWP AVG 0.019	3	All (9)	378,952.80	912,067.10	134,120.20	45,016.79	10,968.02	94.38	77.03
LWP AVG 0.028	4	All (3)	350,015.50	1,031,761.00	144,970.60	38,662.37	10,971.87	99.57	77.93
LWP AVG 0.038	5	All (3)	373,958.20	1,377,098.00	177,550.90	32,344.86	10,923.26	99.77	77.53
RWP 0.000+0.0	1	1	857,353.00	464,829.00	135,540.00	53,113.60	11,282.96	81.90	63.60

RWP 0.038+0	5	1	585,230.80	775,128.20	112,460.30	37,692.17	11,048.73	98.70	72.10
RWP 0.038+6	5	4	574,127.80	804,773.10	139,678.30	35,359.04	11,064.22	92.60	74.90
RWP 0.038+12	5	2	607,341.10	768,003.50	120,059.70	35,557.96	11,046.91	99.40	72.30
RWP 0.038+24	5	3	602,137.60	724,614.30	118,353.00	38,318.16	11,084.27	98.70	73.00
RWP AVG 0.000	1	All (3)	862,324.40	442,373.10	137,575.30	52,930.90	11,323.06	83.57	63.70
RWP AVG 0.009	2	All (5)	634,217.80	678,364.20	134,213.20	36,580.20	11,214.42	88.72	67.20
RWP AVG 0.019	3	All (7,8)	621,149.60	627,530.30	109,485.30	28,377.30	11,124.37	94.21	70.76
RWP AVG 0.028	4	All (3)	624,605.20	527,970.00	111,322.80	37,692.17	11,137.13	98.03	71.33
RWP AVG 0.038	5	All (4)	592,209.30	768,129.80	122,637.80	36,731.83	11,061.03	97.35	73.08

Table B2. ELSYM5 Strain Results at Different Pavement Locations

Location	Strain Type	Strains Under Load Plate		
		0 in	0.1 in	9.4 in
LWP 0.028+0.0	EXX	-56.40	-52.57	4.90
	EYY	-56.40	-52.57	4.90
	EZZ	-116.40	-120.40	-83.13
LWP 0.009-3.2	EXX	-65.53	-61.90	19.78
	EYY	-65.53	-61.90	19.78
	EZZ	-74.72	-78.54	-74.61
LWP AVG 0.000	EXX	-54.75	-32.40	11.16
	EYY	-54.75	12.86	11.16
	EZZ	-94.42	8.59	-74.66
LWP AVG 0.009	EXX	-65.73	-62.05	18.96
	EYY	-65.73	-62.05	18.96
	EZZ	-77.47	-81.34	-75.39
LWP AVG 0.019	EXX	-55.15	-51.51	6.76
	EYY	-55.15	-51.51	6.76
	EZZ	-105.00	-108.80	-77.65
LWP AVG 0.028	EXX	-57.22	-53.37	4.28
	EYY	-57.22	-53.37	4.28
	EZZ	-116.40	-120.40	-83.04
LWP AVG 0.038	EXX	-52.07	-48.55	1.23
	EYY	-52.07	-48.55	1.23
	EZZ	-109.80	-113.50	-76.33
RWP 0.000+0.0	EXX	-41.03	-38.90	22.83
	EYY	-41.03	-38.90	22.83
	EZZ	-30.55	-32.79	-47.26
RWP 0.038+0	EXX	-45.90	-43.29	11.76
	EYY	-45.90	-43.29	11.76
	EZZ	-57.78	-60.53	-53.37
RWP 0.038+6	EXX	-45.94	-43.30	10.94
	EYY	-45.94	-43.30	10.94
	EZZ	-59.98	-62.75	-53.98
RWP 0.038+12	EXX	-45.19	-42.65	12.05
	EYY	-45.19	-42.65	12.05
	EZZ	-54.63	-57.30	-51.80
RWP 0.038+24	EXX	-45.86	-43.28	13.17
	EYY	-45.86	-43.28	13.17
	EZZ	-55.15	-57.87	-53.11
RWP AVG 0.000	EXX	-41.58	-39.44	23.87
	EYY	-41.58	-39.44	23.87
	EZZ	-29.79	-32.05	-47.97
RWP AVG 0.009	EXX	-45.75	-43.22	14.73
	EYY	-45.75	-43.22	14.73
	EZZ	-51.15	-53.82	-52.35

RWP AVG 0.019	EXX	-48.75	-46.14	16.01
	EYY	-48.75	-46.14	16.01
	EZZ	-49.21	-51.95	-53.42
RWP AVG 0.028	EXX	-47.10	-44.46	19.99
	EYY	-47.10	-44.46	19.99
	EZZ	-50.54	-53.31	-56.50
RWP AVG 0.038	EXX	-45.70	-43.10	11.96
	EYY	-45.70	-43.10	11.96
	EZZ	-56.86	-59.59	-53.02